Hyeonjin Eun, Peter Gyula Szabo, Darlyn Rehhorn, Seungwoo Lee, Yongheum Jo, Marcus Altmaier, Jinyoung Lee, Xavier Gaona* and Jong-Il Yun*

Uptake of Eu, Th, U, and Pu by granite and biotite gneiss in Korean fresh groundwater under oxidizing and reducing conditions

Abstract: The uptake of Eu, Th, U, and Pu by Korean granite and biotite gneiss was investigated in a series of batch experiments. Experiments were conducted under well-defined redox conditions, *i.e.*, oxidizing (air), mildly reducing (Ar-atmosphere and buffered with hydroquinone, pe + pH ≈ 8–9), and strongly reducing (Ar-atmosphere and buffered with $Na_2S_2O_4$, pe + pH ≈ 0.5–3). Radionuclide concentration, pH and E_h were systematically monitored up to $t \leq 113$ days after the addition of the radionuclide. The natural content of Eu, Th and U in pristine granite and biotite gneiss materials was quantified by means of alkaline fusion. Eu exhibited moderate sorption on biotite gneiss displaying higher distribution ratios (R_d) compared to granite. This observation was possibly explained by the affinity of Ln(III)/An(III) towards biotite mineral absent in the investigated granite material. Strong sorption was observed for Th, U, and Pu in reducing systems where the predominance of the +IV oxidation state is expected. For these three systems, the strength of the uptake follows the order R_d(Pu(IV)) > R_d(U(IV)) > R_d(Th(IV)), consistent with the hydrolysis strength of the corresponding aquo-ions. A significantly weaker sorption was observed for U and Pu under oxidizing conditions, although R_d values are manifestly higher for Pu than U. Thermodynamic calculations for the oxidizing conditions predicted the predominance of U(VI) and Pu(V)/Pu(IV), explaining observed differences in retention under oxidizing conditions. These results contribute to a quantitative description and a better understanding of the retention of redox-sensitive radionuclides in crystalline host rocks. Emphasis is placed on the importance of utilizing both redox-stable probes (*e.g.*, Eu, Th) and redox-sensitive actinides (*e.g.*, U, Pu), as well as well-defined redox conditions for accurate predictions of radionuclide retention.

Keywords: sorption; actinide elements; europium; granite; biotite gneiss; redox conditions

Hyeonjin Eun and Peter Gyula Szabo contributed equally and should be regarded as co-first authors.

***Corresponding authors: Xavier Gaona**, Institute for Nuclear Waste Disposal (INE), Karlsruhe Institute of Technology, Karlsruhe 76344, Germany, E-mail: xavier.gaona@kit.edu. https://orcid.org/0000-0002-0787-200X; and **Jong-Il Yun**, Department of Nuclear and Quantum Engineering, KAIST, 291 Daehak-ro, Yuseong-gu, Daejeon 34141, Republic of Korea, E-mail: jiyun@kaist.ac.kr. https://orcid.org/0000-0001-8629-2259

Hyeonjin Eun and Seungwoo Lee, Department of Nuclear and Quantum Engineering, KAIST, 291 Daehak-ro, Yuseong-gu, Daejeon 34141, Republic of Korea, E-mail: hjeun@kaist.ac.kr (H. Eun), seungwoo.lee17@kaist.ac.kr (S. Lee). https://orcid.org/0009-0005-3410-7644 (H. Eun). https://orcid.org/0009-0004-1483-4441 (S. Lee)

Peter Gyula Szabo, **Darlyn Rehhorn and Marcus Altmaier**, Institute for Nuclear Waste Disposal (INE), Karlsruhe Institute of Technology, Karlsruhe 76344, Germany, E-mail: peter.szabo@kit.edu (P.G. Szabo), darlyn.rehhorn@kit.edu (D. Rehhorn), marcus.altmaier@kit.edu (M. Altmaier). https://orcid.org/0009-0003-8790-6613 (P.G. Szabo)

Yongheum Jo, Department of Nuclear Engineering, Hanyang University, 222 Wangsimni-ro, Seoul 04763, Republic of Korea, E-mail: yongheumjo@hanyang.ac.kr. https://orcid.org/0000-0003-2425-389X

Jinyoung Lee, Eco-technology Research Team, Hyundai Engineering & Construction, 75 Yulgok-ro, Jongno-gu, Seoul 03058, Republic of Korea, E-mail: jinyounglee@hdec.co.kr. https://orcid.org/0009-0003-8273-1551

1 Introduction

Numerous countries consider deep crystalline formations as one of the candidate host rocks for high-level radioactive waste (HLW) disposal.[1–6] Among them, countries like Finland and Sweden have already selected sites or begun constructing the HLW disposal facility in crystalline host rock.[7] In South Korea, crystalline granite and biotite gneiss, renowned for their robustness, structural integrity, and low permeability, are being considered as potential host rock materials for disposal facilities.[8–10] Despite the strong protection offered by the engineered barrier system, which includes metallic canister and buffer material, the failure of both components would ultimately allow radionuclides to come into contact with groundwater. The ingress of groundwater in granite environments may occur through fractures and cracks, and accordingly, it is necessary to investigate the solution chemistry and retention properties of radionuclides under such conditions.[11–13]

Sorption of the radionuclides in the far-field is an important process contributing to the safety concept of disposal facilities. The generic term "sorption" embraces several underlying retention mechanisms, including outer-sphere sorption, inner-sphere complexation, incorporation/solid-solution formation, or surface precipitation.[14] Accordingly, the unequivocal identification of the sorption mechanisms is challenging, especially for sparingly soluble radionuclides such as actinides under reducing conditions.

The presence of natural stable- and radionuclides in natural crystalline rocks should be considered in the interpretation of sorption phenomena.[15–18] Korean granite and biotite gneiss have been reported to contain up to 2, 40, and 65 mg kg^{-1} of Eu, U, and Th, respectively.[19–21] Measurements of sorption distribution ratios using elemental quantitative analysis methods such as ICP-MS are affected by the elements present in the pristine matrix. It is thus beneficial to quantify the content of stable nuclides and radionuclides in the original material as well as the concentrations leached to the groundwater solution before the addition of the radionuclides in the sorption experiments. When dealing with other radioisotopes (*e.g.*, ^{152}Eu, ^{228}Th, ^{233}U) and depending on the accessibility of the natural stable nuclides and radionuclides in the pristine material, isotopic exchange processes may need to be taken into account.

Actinides like U and Pu play pivotal roles in the HLW disposal,[22,23] exhibiting redox-sensitive behavior that dictates their chemistry based on the redox conditions.[24–28] In reducing conditions expected after the post closure of repository, U(IV) and Pu(III/IV) are expected to dominate the aqueous chemistry of U and Pu. However, under oxidizing conditions, U(VI) will prevail, whereas Pu is found as Pu(IV), Pu(V), or Pu(VI), depending upon pH and E_h conditions.

In general, tri- and tetravalent actinides exhibit strong sorption,[14,29–31] whereas hexavalent actinides are known to be more mobile in crystalline rock media.[32–34] Actinides typically exist as cations at lower pH and turn into neutral (+III and +IV) or anionic (+V and +VI) species as pH increases by stepwise hydrolysis reactions.[24] In conjunction with the evolution of the surface charge of the rock material, this leads to a differential sorption behavior as a function of pH and the oxidation state of actinides.[35]

A joint study by KAIST, Hyundai E&C from South Korea, and KIT from Germany aimed to quantitatively investigate the sorption characteristics of actinides with various oxidation states (+III to +VI) with granite and biotite gneiss, representative crystalline rocks in South Korea. Eu(III) was utilized as a chemical analogue of trivalent actinides (Pu(III), Am(III), and Cm(III)). Th(IV), U(IV), and Pu(IV) were used to represent tetravalent actinides, while U(VI) was used for representing hexavalent actinides (U(VI) and Pu(VI)).

This independent and collaborative efforts between KAIST and KIT enhance the reliability of sorption data, crucial for the safety assessment of disposal facilities hosted in crystalline bedrocks.

2 Experimental

2.1 Chemicals and radiotracers

Experiments were independently conducted at KAIST and KIT. The experiments were conducted at $T = (22 \pm 2)$ °C either in air (oxidizing samples) or under Ar atmosphere (reducing samples, O_2 < 2 ppm). Solutions were prepared with ultra-pure water (18.2 MΩ cm at (22 ± 2) °C, 4 ppb TOC) purified with Milli-Q equipment (Milli-Q Advantage A10 with 0.22 µm Millipore Millipak® 40 filter). Before use, Milli-Q water was flushed with Ar for > 1 h in order to purge the dissolved O_2 and CO_2.

NaOH, HCl (both Titrisol), $C_6H_6O_2$ (hydroquinone, HQ, p.a.), $Na_2S_2O_4$ (sodium dithionite, >87 %), concentrated HNO_3 (Supra- and Ultrapure, and ≥99.999 % trace metals basis), $EuCl_3{\cdot}6H_2O$(s) (99.9 % trace metals basis, stable isotopes) and $Th(NO_3)_4{\cdot}6H_2O$(s) (99 %, ^{232}Th) were obtained from Merck. $UO_2(NO_3)_2{\cdot}6H_2O$(s) used at KAIST was obtained from Fluka (puriss. p.a. ACS, natural isotopic abundance), and $UO_2(NO_3)_2{\cdot}6H_2O$(s) used at KIT was obtained from Merck (99 %). The isotopic composition of the Pu(VI) stock used was 99.4 wt% ^{242}Pu, 0.58 wt% ^{239}Pu, 0.005 wt% ^{238}Pu and 0.005 wt% ^{241}Pu. Initial Pu and U stock solutions ($[Pu]_{tot} = 5.6 \times 10^{-2}$ M in 3 M $HClO_4$; $[U]_{tot} = 8.8 \times 10^{-3}$ M in 0.2 M HCl) were diluted with 0.2 M HCl to $[Pu]_{tot} = 4.8 \times 10^{-7}$–$1.6 \times 10^{-7}$ M and $[U]_{tot} = 5.1 \times 10^{-5}$–$5.1 \times 10^{-6}$ M. These diluted stock solutions were used for the preparation of all sorption samples. Although Pu(IV) and U(IV) are expected to prevail in the sorption experiments conducted under reducing conditions, the use of the +VI oxidation state instead of the +IV was preferred for both radionuclides to avoid largely oversaturated conditions that may result in the formation of intrinsic An(IV) colloids.[27,36–39]

2.2 Solid materials and pore waters used in sorption experiments

Granite and biotite gneiss cores were drilled at a depth of 744 m into the ground near the south-eastern coast of the Korean Peninsula (Gyeongsangbuk-do, South Korea), while biotite gneiss was drilled at a depth of 82 m (Gyeonggi-do, South Korea).[40] They were finely crushed with a jaw crusher (Pulverisette 1, Fritsch) and an iron disk mill (Pulverisette 13, Fritsch). The cumulative particle size distribution (Q_3) is measured by the particle size analyser (HELOS, Sympatec

GmbH) and the results are shown in Figure S4 in the Supplementary Material. For granite and biotite gneiss, the median diameters ($D_{50\,\%}$) are 43.1 and 35.7 µm and the upper ends of the particle size ($D_{99\,\%}$) are 263 and 233 µm, respectively.

Groundwater was collected from 130 m below sea level near the south-eastern coast of the Korean Peninsula (Gyeongsangbuk-do, South Korea). The groundwater was divided into two batches: one equilibrated with air in Kautex bottles (Korean Fresh Groundwater under Oxidizing condition, KFGO), and the other stored in pressurized stainless-steel cylinders (SMGI, Co., Ltd) filled with Ar to maintain an anoxic condition (Korean Fresh Groundwater under Reducing condition, KFGR). After equilibrium was reached (*ca.* 5 months), the precipitate from the two groundwater solutions was filtered using filter paper (No. 1 Qualitative, Whatman). The target pH was determined based on the equilibrium state achieved under laboratory conditions, and the reference pe values were set arbitrarily (±500 mV) to simulate oxidizing and reducing environments. KFGO and KFGR were shipped from KAIST to KIT in Kautex flasks and pressurized stainless-steel cylinders, respectively. Once at KIT, KFGR solutions were transferred to Kautex bottles and stored inside an Ar-glovebox. The elemental composition of KFGO and KFGR groundwaters was measured by ICP-OES (Optima 8300, Perkin Elmer) and IC (ICS-6000, Thermo Fisher) and the results are provided in Table 1.

The content of natural Eu, Th, and U in pristine granite and biotite gneiss was quantified by means of alkali fusion with KOH at T = 390 °C, followed by ICP-MS measurement after dilution with 2 % HNO_3. To quantify the leaching of natural Eu, Th, and U from the pristine granite and biotite gneiss, these materials were contacted with groundwater at three S/L ratios of 5, 10, and 50 g L^{-1} and shaken for 20 days under oxidizing (air) conditions. The solid and liquid phases were then separated by centrifugation at 10,600 g for 30 min and the concentration of the liquid phase was measured by ICP-MS (iCAP RQ, Thermo Fisher). The detection limits were [Eu] ≈ 1×10^{-10} M, [Th] ≈ 1×10^{-12} M, and [U] ≈ 1×10^{-10} M.

2.3 pH and E_h measurements

The pH values were determined with combination pH electrodes (type Orion ROSS, Thermo Scientific) calibrated with standard pH buffer solutions (7 ≤ pH ≤ 12, Merck). Redox potentials were determined with combined Pt and Ag/AgCl reference electrodes (Metrohm). Measured potentials were converted to E_h (Standard Hydrogen Electrode: SHE) by considering the potential of Ag/AgCl inner-reference electrode in 3 M KCl at T = 22 °C, *i.e.,* +207 mV. E_h values were converted to pe (pe = $-\log a_{e^-}$) according to $E_h = -(RT/F) \ln(10) \log a_{e^-}$, where R is the ideal gas constant (8.3144 J mol^{-1} K^{-1}) and F is the Faraday constant (96,485.3 C mol^{-1}).

2.4 Sorption experiments

Batch sorption experiments were independently conducted at KAIST and KIT using the same rock-groundwater systems. At KAIST, the experiments were performed in triplicate under oxidizing conditions. The mean values and standard deviations of the triplicates are presented in Tables 2, 3, and 6. At KIT, single-batch sorption experiments were conducted under oxidizing and reducing conditions. The mean values and standard deviations of repeated sampling are presented in Tables 2, 3, and 6.

Sorption samples were prepared by contacting the granite and biotite gneiss with KFGO and KFGR (V_{tot} = 10 mL; in a 20 mL HDPE vial (Wheaton) at KAIST and V_{tot} = 10 mL; in a 15 mL PP conical tube (Sarstedt) at KIT), targeting solid-to-liquid (S/L) ratios of 0.2 g L^{-1} ≤ S/L ≤ 50 g L^{-1}. Reducing agents (2 mM HQ or 2 mM $Na_2S_2O_4$) were added to selected U(VI) and Pu(VI) samples in order to maintain mildly (pe + pH ≈ 9 ± 1) and strongly (pe + pH ≈ 1.5 ± 1) reducing conditions.[25,36,42,43] The oxidation states of U(IV) and Pu(IV) were determined solely from pH and E_h measurements. pH and E_h values were monitored for up to t ≤ 34 days. Acknowledging that E_h measurements of redox-unbuffered systems are clearly less reliable,[44] the same contact times and monitoring steps were considered for the oxidizing samples. Small volumes (20–21 µL) of the diluted radionuclide stock solutions were spiked to the suspensions, aiming at $[Eu]_0 = 1 \times 10^{-8}$ M, $[^{232}Th]_0 = 1 \times 10^{-9}$ M, $[^{238}U]_0 = 1 \times 10^{-6}$, 1×10^{-7}, 1×10^{-8} M and $[^{242}Pu]_0 = 1 \times 10^{-9}$, 3×10^{-10} M.

Table 1: Elemental composition of Korean Fresh Groundwater under Oxidizing condition (KFGO) and Korean Fresh Groundwater under Reducing condition (KFGR) measured by ICP-OES for metals and SiO_2 and IC for anions.[40] All values in micromolar (µM), except otherwise indicated. The standard deviation of the 3 repeated measurements is within 2 %.

Groundwater	pH	K	Na	Ca	Mg	SiO_2	Sr	Mn	F	Cl	SO_4
KFGO	8.04	72.9	1,200	928	353	904	0.263	0.359	9.42	578	1,050
KFGR	9.22										

Table 2: Experimentally measured pH and E_h values for the granite and biotite gneiss samples investigated in this work. For KAIST samples, average values and standard deviations (σ) of the triplicated samples after sorption (20 days) are shown. For KIT samples, average values were calculated over a time period of $t \leq 153$ days, with uncertainties calculated as standard deviation (σ) of mean values. E_h values are converted into pe as described in the text. (pe + pH) values are provided as a measure of the redox conditions in the system.[41]

Eu samples/S/L (g L^{-1})	pH	E_h (mV)	pe	(pe + pH)	Laboratory
Granite/1 (air)	(7.87 ± 0.01)	(388 ± 5)	(6.6 ± 0.1)	(14.5 ± 0.1)	KAIST
Biotite gneiss/1 (air)	(8.02 ± 0.04)	(391 ± 2)	(6.6 ± 0.0)	(14.6 ± 0.0)	KAIST
Granite/10 (air)	(7.87 ± 0.02)	(391 ± 5)	(6.6 ± 0.1)	(14.5 ± 0.1)	KAIST
Biotite gneiss/10 (air)	(8.04 ± 0.04)	(389 ± 2)	(6.6 ± 0.0)	(14.6 ± 0.0)	KAIST
Th samples/S/L (g L^{-1})	**pH**	**E_h (mV)**	**pe**	**(pe + pH)**	**Laboratory**
Granite/0.2 (air)	(7.89 ± 0.06)	(388 ± 6)	(6.6 ± 0.1)	(14.5 ± 0.1)	KAIST
Biotite gneiss/0.2 (air)	(7.89 ± 0.04)	(388 ± 2)	(6.6 ± 0.0)	(14.5 ± 0.0)	KAIST
Granite/1 (air)	(7.88 ± 0.02)	(391 ± 1)	(6.6 ± 0.0)	(14.5 ± 0.0)	KAIST
Biotite gneiss/1 (air)	(7.92 ± 0.02)	(390 ± 1)	(6.6 ± 0.0)	(14.5 ± 0.0)	KAIST
Granite/10 (air)	(7.92 ± 0.03)	(385 ± 4)	(6.5 ± 0.1)	(14.4 ± 0.1)	KAIST
Biotite gneiss/10 (air)	(8.02 ± 0.01)	(392 ± 2)	(6.6 ± 0.0)	(14.6 ± 0.0)	KAIST
U samples/S/L (g L^{-1})	**pH**	**E_h (mV)**	**pe**	**(pe + pH)**	**Laboratory**
Granite/5 (air)	(7.96 ± 0.02)	(392 ± 2)	(6.6 ± 0.0)	(14.6 ± 0.0)	KAIST
Biotite gneiss/5 (air)	(8.04 ± 0.02)	(391 ± 3)	(6.6 ± 0.1)	(14.6 ± 0.1)	KAIST
Granite/50 (air)	(8.31 ± 0.70)	(390 ± 3)	(6.6 ± 0.1)	(14.9 ± 0.7)	KAIST
Biotite gneiss/50 (air)	(8.16 ± 0.03)	(391 ± 1)	(6.6 ± 0.0)	(14.8 ± 0.0)	KAIST
Granite/5 (air)	(7.8 ± 0.3)	(423 ± 26)	(7.2 ± 0.4)	(14.9 ± 0.2)	KIT
Biotite gneiss/5 (air)	(7.9 ± 0.2)	(423 ± 25)	(7.2 ± 0.4)	(15.1 ± 0.3)	KIT
Granite/50 (air)	(7.9 ± 0.2)	(434 ± 26)	(7.4 ± 0.4)	(15.2 ± 0.3)	KIT
Biotite gneiss/50 (air)	(8.1 ± 0.1)	(429 ± 23)	(7.3 ± 0.4)	(15.3 ± 0.4)	KIT
Granite/0.2 ($Na_2S_2O_4$)	(9.1 ± 0.2)	–(521 ± 30)	–(8.9 ± 0.5)	(0.2 ± 0.5)	KIT
Biotite gneiss/0.2 ($Na_2S_2O_4$)	(9.0 ± 0.1)	–(509 ± 42)	–(8.7 ± 0.7)	(0.3 ± 0.7)	KIT
Granite/1 ($Na_2S_2O_4$)	(9.0 ± 0.1)	–(496 ± 41)	–(8.5 ± 0.7)	(0.6 ± 0.7)	KIT
Biotite gneiss/1 ($Na_2S_2O_4$)	(9.0 ± 0.1)	–(498 ± 37)	–(8.5 ± 0.6)	(0.5 ± 0.6)	KIT
Pu samples/S/L (g L^{-1})	**pH**	**E_h (mV)**	**pe**	**(pe + pH)**	**Laboratory**
Granite/50 (air)	(7.9 ± 0.1)	(452 ± 23)	(7.7 ± 0.4)	(15.6 ± 0.4)	KIT
Biotite gneiss/50 (air)	(8.1 ± 0.1)	(451 ± 21)	(7.7 ± 0.4)	(15.7 ± 0.4)	KIT
Granite/1 (HQ)	(8.9 ± 0.2)	–(11 ± 76)	(0.3 ± 1.5)	(9.2 ± 1.6)	KIT
Biotite gneiss/1 (HQ)	(8.8 ± 0.2)	–(39 ± 86)	(0.0 ± 1.7)	(8.9 ± 1.9)	KIT
Granite/10 (HQ)	(8.9 ± 0.2)	–(14 ± 86)	–(0.2 ± 1.5)	(8.6 ± 1.6)	KIT
Biotite gneiss/10 (HQ)	(8.8 ± 0.2)	–(46 ± 136)	–(1.1 ± 1.8)	(7.8 ± 1.9)	KIT
Granite/10 ($Na_2S_2O_4$)	(9.0 ± 0.3)	–(371 ± 157)	–(5.9 ± 2.7)	(3.1 ± 2.5)	KIT
Biotite gneiss/10 ($Na_2S_2O_4$)	(9.0 ± 0.2)	–(365 ± 159)	–(5.8 ± 2.7)	(3.1 ± 2.6)	KIT

At KAIST, blank samples were prepared in triplicate to accurately measure the initial concentration and account for the amount sorbed onto the container wall. In addition, a leaching experiment from the crushed rocks was performed to accurately estimate the initial concentration ($[RN]_0$). After 20 days of contact time, the suspensions were centrifugated for 30 min at 10,600 g to separate the aqueous phase. For ICP-MS measurements at KAIST, 70 % HNO_3 (≥99.999 % trace metals basis) was spiked in the blank KFGO to prepare a 2 % nitric acid groundwater solution. Both calibration standards and samples were diluted with this solution to lower the detection limits by minimizing the matrix effects.[45] pH and E_h were measured once after sorption.

At KIT, after the addition of radionuclides, pH, E_h, $[RN]_{aq}$ and total inorganic carbon (TIC) were monitored for up to $t \leq 113$ days. $[RN]_{aq}$ and TIC were characterized after ultrafiltration with 10 kD filters (Nanosep®, Pall Life Sciences; pore size ≈ 2–3 nm). The filtrated solutions were diluted with 2 % HNO_3 (Suprapur).

U and Pu concentrations were determined by sector field inductively coupled plasma mass spectrometry (SF-ICP-MS; type Element XR, Thermo Fisher) at KIT. Eu, Th and U

Table 3: Experimental conditions in the batch sorption samples investigated in this work. Samples with a contact time of 20 days were performed at KAIST and samples with ≤113 days were performed at KIT.

RN	Redox condition	S/L (g L^{-1})	log ($[RN]_0$ (M))	Redox buffer	pH	V_{tot} (mL)	Number of samples	Contact time (days)
Eu	Oxidizing	1	7.5	–	7.9	10	6 (triplicate)	20
Eu	Oxidizing	10	7.5	–	8.0	10	6 (triplicate)	20
^{232}Th	Oxidizing	0.2	9	–	7.9	10	6 (triplicate)	20
^{232}Th	Oxidizing	1	9	–	7.9	10	6 (triplicate)	20
^{232}Th	Oxidizing	10	9	–	8.0	10	6 (triplicate)	20
^{238}U	Oxidizing	5	6	–	8.0	10	6 (triplicate)	20
^{238}U	Oxidizing	50	6	–	8.2	10	6 (triplicate)	20
^{238}U	Oxidizing	5	7	–	8.0	10	2 (single)	≤112
^{238}U	Oxidizing	50	7	–	8.0	10	2 (single)	≤112
^{238}U	Reducing	0.2	8	2 mM $Na_2S_2O_4$	9.2	10	2 (single)	≤112
^{238}U	Reducing	1	8	2 mM $Na_2S_2O_4$	9.2	10	2 (single)	≤112
^{242}Pu	Oxidizing	50	9.5	–	8.0	10	2 (single)	≤112
^{242}Pu	Reducing	1	9	2 mM HQ	9.2	10	2 (single)	≤113
^{242}Pu	Reducing	10	9	2 mM HQ	9.2	10	2 (single)	≤113
^{242}Pu	Reducing	10	9	2 mM $Na_2S_2O_4$	9.2	10	2 (single)	≤113

concentrations were quantified by inductively coupled plasma mass spectrometry (ICP-MS; iCAP RQ, Thermo Fisher) at KAIST. Detection limits were determined as three times the standard deviation of the blank signal, resulting in [Eu] ≈ 1×10^{-10} M, [Th] ≈ 1×10^{-12} M, [U] ≈ 1×10^{-10} M (ICP-MS), [U] ≈ 3×10^{-11} M (SF-ICP-MS) and [Pu] ≈ 4×10^{-13} M. TIC analyses were performed using an Analytik Jena multi/c 2100 S instrument. At KIT, the volume in each batch sample was systematically restored with the corresponding groundwater after each sampling. Experimental conditions of all sorption samples investigated in this work are summarized in Table 3.

The sorption of Eu, Th, U, and Pu was evaluated in terms of the distribution ratio, R_d (L kg^{-1}), calculated as the ratio of radionuclide concentration in the solid ($[RN]_{solid}$, in mol kg^{-1}) and aqueous ($[RN]_{aq}$, in M) phases:

$$R_d = \frac{[RN]_{solid}}{[RN]_{aq}} = \frac{[RN]_0 - [RN]_{aq}}{[RN]_{aq}} \times \frac{V}{m} \quad (1)$$

where $[RN]_0$ is the initial concentration of the radionuclide in solution, V is the volume of the sample (L), and m is the mass of crushed rock (kg).

2.5 Solid phase characterization

Granite and biotite gneiss materials were characterized by XRD before and after conducting the sorption experiments with a D8 Advance (Bruker AXS) diffractometer (CuKα radiation) equipped with an energy-dispersive detector. A small fraction of the solid materials (1–2 mg) was deposited on a crystal silicon plate either as a suspension with ethanol or as a dry powder, and covered with an air-tight dome. Diffractograms were collected in the range of 5° ≤ 2θ ≤ 90°, with a step size of 0.011° and a counting time of 0.5 s per step. Raw data were evaluated using the Bruker AXS Diffrac^{Plus} EVA software. XRD patterns were compared to reference data available within the JCPDS database.[46]

To quantitatively analyse the composition of granite and biotite gneiss, the XRD data were analysed using the Rietveld method with Siroquant ver. 4.0 software and XRF (PW2400, Philips) analysis was performed. The XRF measurements were made in a vacuum (2.5 Pa) with a voltage of 24–40 kV and a current of 50–80 mA. Ten reference minerals (Brammer Standard Company) were used for calibration.

3 Results and discussion

3.1 Solid and aqueous phase characterization

Figures 1 and 2 show the diffractograms of granite and biotite gneiss materials, respectively, before and after sorption experiments. Both materials show main reflections of quartz and clay components (see Table 4), in line with the elemental composition quantified by XRF (Table 5). Similar patterns are observed before and after conducting the sorption experiments, thus indicating that no significant changes were triggered by sorption processes. For the biotite gneiss system, some differences arise for the sample containing Pu under reducing conditions. Whilst the position of most

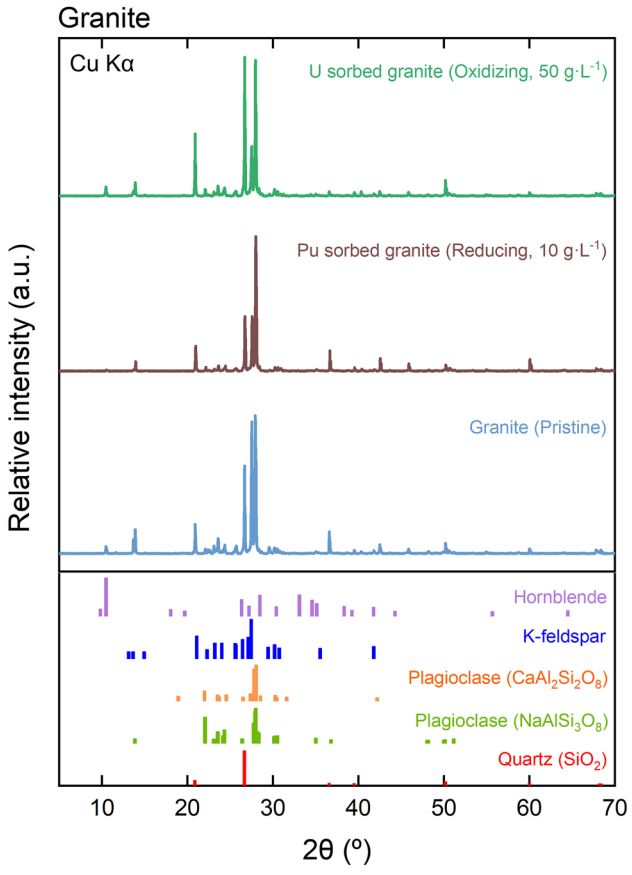

Figure 1: XRD diffractograms of the investigated granite material, before and after conducting the sorption experiments. Samples after the sorption corresponding to U under oxidizing conditions (50 g L^{-1}) and Pu under reducing conditions (buffered with HQ, 10 g L^{-1}). Symbols correspond to the patterns reported for quartz (SiO_2, PDF 85-0795), plagioclase ($CaAl_2Si_2O_8$, PDF 41-1486; $NaAlSi_3O_8$, PDF 84-0753), K-feldspar ($KAlSi_3O_8$, PDF 22-0688) and hornblende ($Ca_2(Mg, Fe, Al)_5(Al, Si)_8O_{22}(OH)_2$, PDF 71-1063) reference materials.

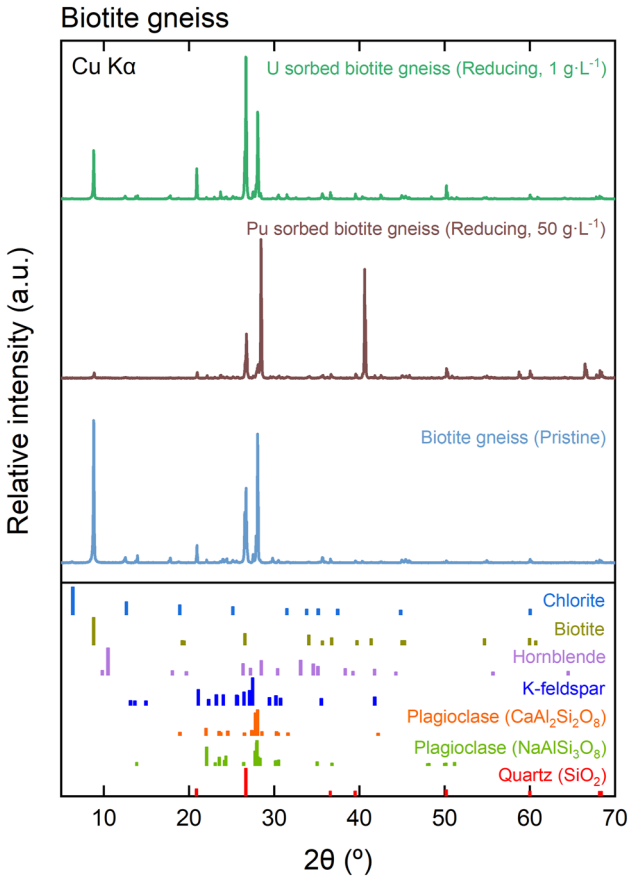

Figure 2: XRD diffractograms of the investigated biotite gneiss material, before and after conducting the sorption experiments. Samples after the sorption corresponding to U under reducing conditions (1 g L^{-1}) and Pu under reducing conditions (buffered with HQ, 10 g L^{-1}). Symbols correspond to the patterns reported for quartz (SiO_2, PDF 85-0795), plagioclase ($CaAl_2Si_2O_8$, PDF 41-1486; $NaAlSi_3O_8$, PDF 84-0753), K-feldspar ($KAlSi_3O_8$, PDF 22-0688) and hornblende ($Ca_2(Mg, Fe, Al)_5(Al, Si)_8O_{22}(OH)_2$, PDF 71-1063) reference materials.

features remains the same, differences can be observed in the relative intensities of some of these reflections (*e.g.*, weaker intensity at ~9°, or greater intensity at ~40°). This observation could be explained by a favoured crystal orientation occurring in the process of sample preparation for XRD measurements.

Alkaline fusion experiments confirmed the presence of natural Eu, Th and U in pristine granite and biotite gneiss materials (see Table 6). These values are in line with previous studies reporting the concentration of these elements in Korean granitic materials.[19,20]

For granite and biotite gneiss, leaching tests resulted in Eu and Th concentrations below the detection limit ([Eu] ≤ 1×10^{-10} M, [Th] ≤ 1×10^{-12} M), whereas U concentrations (under oxidizing conditions) were quantified as [U] = (1.8 ± 0.9) nM in granite and [U] = (0.4 ± 0.4) nM in biotite gneiss (Figure S5). In all cases, the leached concentrations are well below the initial concentrations used in the sorption experiments (see Table 3), and thus it is considered that their impact on the quantification of distribution ratios is negligible. No leaching tests were performed for U under reducing conditions, and an analogous behavior as observed for Th is hypothesized, considering the expected predominance of U(IV) under such boundary conditions (see Section 3.3).

3.2 Determination of (pe + pH) and c_{tot}

The E_h and pH of the suspensions with solid materials (granite, biotite gneiss) and groundwaters (KFGO, KFGR) were regularly monitored before and after the addition of radionuclides (see Table 1, and Figures S1 and S2 in the

Table 4: Crystallographic compositions of granite and biotite gneiss materials (in wt%) as characterized by XRD with Rietveld method. The relative error is ~5–10 %.

Material	Quartz	Plagioclase	K-feldspar	Biotite	Chlorite	Hornblend
Granite	33.9	35.8	26.8	–	–	3.5
Biotite gneiss	44.7	34.3	4.1	16.6	0.3	–

Table 5: Elemental composition of granite and biotite gneiss materials (in wt%) as characterized by XRF. The standard deviation of 5 repeated measurements is within 2 %.

Material	Al_2O_3	CaO	Fe_2O_3	K_2O	MgO	MnO	Na_2O	P_2O_5	SiO_2	TiO_2	LOI[a]	Total
Granite	12.9	0.22	1.47	4.80	0.13	0.04	3.65	–	76.17	0.08	0.54	100.0
Biotite gneiss	14.4	2.17	5.73	3.40	1.61	0.04	2.40	0.06	68.37	1.25	0.55	100.0

[a]Loss on ignition.

Table 6: Concentration of natural Eu, Th and U quantified in the pristine granite and biotite gneiss materials investigated in this work.

Material	Eu (ppm/mol kg^{-1})	Th (ppm/mol kg^{-1})	U (ppm/mol kg^{-1})
Granite	$(0.27 \pm 0.02)/(1.8 \pm 0.1) \times 10^{-6}$	$(11.8 \pm 0.6)/(5.1 \pm 0.3) \times 10^{-5}$	$(1.6 \pm 0.1)/(6.5 \pm 0.4) \times 10^{-6}$
Biotite gneiss	$(1.1 \pm 0.1)/(7.2 \pm 0.7) \times 10^{-6}$	$(92 \pm 5)/(4.0 \pm 0.2) \times 10^{-4}$	$(2.6 \pm 0.2)/(1.1 \pm 0.1) \times 10^{-5}$

Supplementary Material). E_h values measured for granite and biotite gneiss suspensions with KFGO are consistently oxidizing ($E_h \approx 400$–450 mV), though slightly lower than the reference E_h (500 mV). As discussed above, redox measurements in weakly buffered redox systems should be taken with precaution, and thus these values are considered to qualitatively support the prevalence of oxidizing conditions in the samples. Figures S2a and S2b show the experimental pH and E_h values, respectively, measured for $t \leq 148$ days under reducing conditions, defined either by HQ or $Na_2S_2O_4$. The experimental (pe + pH) values are in line with redox conditions reported in the literature for analogous systems.[25,28,36,39,47] Slightly increased (pe + pH) values were determined for Pu samples equilibrated in $Na_2S_2O_4$, although very reducing conditions were retained throughout the complete sorption experiments. We attribute this effect to the known instability of $Na_2S_2O_4$ in acidic to weakly alkaline conditions, which might be also accentuated by the higher S/L ratios used in the Pu experiments (10 g L^{-1}), compared to the experiments in the U system containing also $Na_2S_2O_4$ (1 g L^{-1}).

Carbonate concentrations in the oxidizing and reducing systems were determined by means of TIC measurements. Very similar values were found for both systems, *i.e.*, $C_{tot,ox} = (1.5 \pm 0.2) \times 10^{-4}$ M and $C_{tot,red} = (1.8 \pm 0.5) \times 10^{-4}$ M, with uncertainties calculated as the standard deviation of mean values. For comparison purposes, Figure S3 in the Supplementary Material shows the calculated carbonate concentration in equilibrium with atmospheric CO_2(g) ($P_{CO_2} = 3.13 \times 10^{-4}$ atm) within a pH range of 5–10. The figure indicates that experimentally measured values of C_{tot} in oxidizing conditions (air) are slightly below but in line with predictions based on thermodynamic calculations. Carbonate is a relevant ligand in the U and Pu systems, and thus C_{tot} values determined in this work have been considered for the calculation of the *Pourbaix* diagrams shown in Section 3.3 and corresponding implications for sorption phenomena.

3.3 Thermodynamic calculations. Comparison with experimental (pe + pH) values

Figure 3 shows the experimentally measured pH and E_h values of the investigated systems in the corresponding *Pourbaix* diagrams. Thermodynamic calculations are performed using the current NEA-TDB thermodynamic selection[26] for Th, U, and Pu, and using the ThermoChimie database ver. 11a for Eu. In order to accurately reproduce the boundary conditions in oxidizing and reducing systems, each *Pourbaix* diagram has been calculated at $P_{CO_2} = 3.13 \times 10^{-4}$ atm (Figure 3a, b, c, and e) and

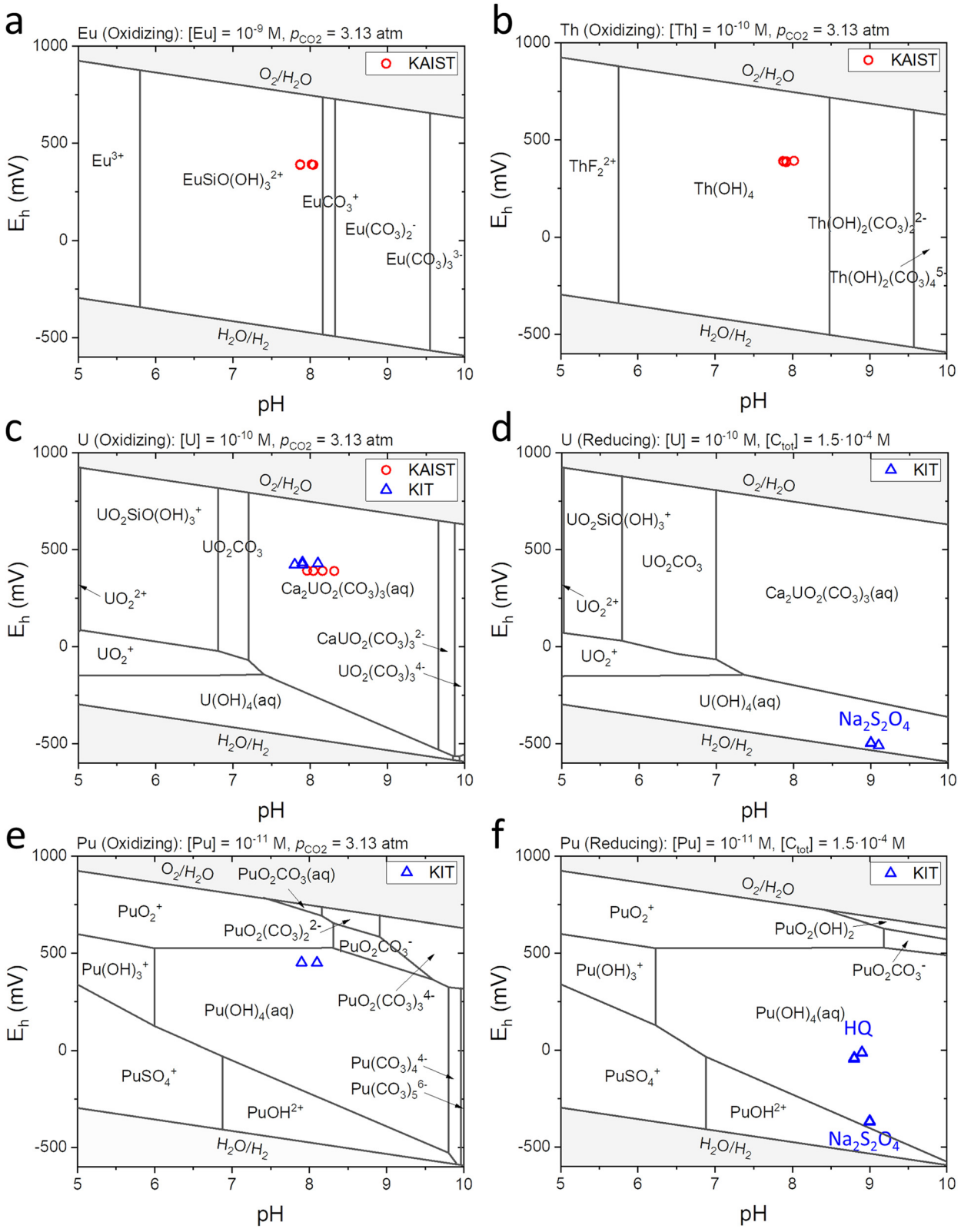

Figure 3: Pourbaix diagrams of (a) [Eu] = 1×10^{-9} M (oxidizing); (b) [Th] = 1×10^{-10} M (oxidizing); (c) [U] = 1×10^{-10} M (oxidizing); (d) [U] = 1×10^{-10} M (reducing); (e) [Pu] = 1×10^{-11} M (oxidizing); (f) [Pu] = 1×10^{-11} M (reducing) in KFGO and KFGR. For the oxidizing conditions (a), (b), (c), and (e), the partial pressure of carbon dioxide was 3.13×10^{-4} atm. For the reducing conditions (d) and (f), the total inorganic carbon concentration was 1.5×10^{-4} M. The precipitation of ions except for the target elements were ignored. The composition of groundwater is shown in Table 1. The experimental conditions from KAIST are represented by red circles, while those from KIT are shown with blue triangles. Calculations for Eu were performed using the ThermoChimie v.11a database and calculations for Th, U, and Pu were performed based on the NEA-TDB thermodynamic selection[26] for Th, U, and Pu.

$C_{tot,red}$ = 1.5 × 10^{-4} M (Figure 3d and f), *i.e.*, considering the carbonate concentrations experimentally determined for oxidizing and reducing systems.

Eu and Th are redox-stable elements whose oxidation states do not change with E_h in the water stability region. Thermodynamic calculations suggest that Eu(III) primarily exists in the form of $EuSiO(OH)_3^{2+}$ in the presence of Si and carbonate concentrations present in the investigated groundwaters. Under these conditions, the speciation of Th(IV) is dominated by $Th(OH)_4$(aq).

The speciation of U in oxidizing conditions (see Figure 3c and d) is dominated by the ternary complex $Ca_2UO_2(CO_3)_3$(aq), as expected for a weakly alkaline system containing moderate concentrations of Ca and carbonate. Figure 3d shows that the speciation of U in reducing conditions defined by $Na_2S_2O_4$ is controlled by U(IV) as $U(OH)_4$(aq). The reduction of U(VI) to U(IV) in strongly reducing conditions defined by $Na_2S_2O_4$ has been previously described in the literature.[25]

The (pe + pH) values experimentally measured in Pu systems equilibrated in air (oxidizing conditions) are located around the redox borderline between Pu(V) (as PuO_2^+) and Pu(IV) (as $Pu(OH)_4$(aq)) (see Figure 3e and f). According to this observation, slight variations in the redox conditions may lead to the predominance of one or the other oxidation state, thus resulting in stronger or weaker retention. In reducing conditions defined by both HQ and $Na_2S_2O_4$, Pu is predominantly expected in the +IV oxidation state as $Pu(OH)_4$(aq). Note that although before the addition of Pu the redox conditions of the KFGR in $Na_2S_2O_4$ were close to −500 mV, a slight increase in the redox potential was observed after the addition of Pu, resulting in $E_h \approx -250$ mV.

3.4 R_d values determined for Eu, Th, U and Pu in oxidizing and reducing systems

Table 7 summarizes the R_d values determined for each of the investigated systems for the uptake of Eu, Th, U and Pu by granite and biotite gneiss materials, as average of 3–4 independent measurements conducted at $t \leq 113$ days for KIT experiments. For KAIST experiments, measurements were performed after 20 days using independent triplicate batch setups. Uncertainties in the table are calculated as the standard deviation of mean values. All measured radionuclide concentrations were below the solubility limits of $EuCO_3OH$(cr), ThO_2(am, hyd), $UO_3{\cdot}2H_2O$(cr) (U, oxidizing conditions), UO_2(am, hyd) (U, reducing conditions) and PuO_2(am, hyd) (Pu, reducing conditions), as calculated with the current NEA-TDB thermodynamic selection (Th, U, and Pu) or the ThermoChimie database (Eu). R_d values are calculated as described in Equation (1), disregarding any contribution from the Eu, Th, and U content in pristine granite and biotite gneiss. This assumption is based on the rather immobile character of these elements in the investigated pristine materials, as hinted by the leaching tests discussed in Section 3.1.

Table 7 and Figures 4 and 5 reflect a relatively large dispersion of the R_d values determined for some radionuclide systems, although clear and consistent trends are observed considering the redox conditions and expected radionuclide oxidation state.

Note that the results obtained for U(VI) in both laboratories (KAIST and KIT) qualitatively agree with each other. A moderate uptake ($2 \leq R_d$ (L kg^{-1}) ≤ 78) is determined for U under oxidizing conditions involving the predominance of U(VI), thus underpinning the weaker sorption expected for this oxidation state. This is also consistent with the strong complexation of U(VI) with carbonate, involving also the formation of the ternary complex $Ca_2UO_2(CO_3)_3$(aq) (see Figure 3).

Eu(III) was used as a chemical analogue for trivalent actinides. Even though Eu(III) has a smaller effective charge than U(VI), Eu(III) showed stronger sorption on crystalline rock surfaces than U(VI) ($1.7 \times 10^2 \leq R_d$ (L kg^{-1}) $\leq 1.7 \times 10^3$). This is because U(VI) forms neutral or negatively charged ternary complexes with carbonate, as mentioned above. It is also consistent with the observation that the sorption of U(VI) is reduced in the presence of carbonate, while no clear inhibition of Eu(III) uptake is seen.[48]

The predominance of U(IV) promoted by reducing conditions leads to a significantly stronger uptake ($3.9 \times 10^3 \leq R_d$ (L kg^{-1}) $\leq 1.2 \times 10^5$), consistent with observations for Th(IV) ($8.2 \times 10^2 \leq R_d$ (L kg^{-1}) $\leq 4.1 \times 10^4$). The uptake of Pu under reducing conditions is also very strong ($1.6 \times 10^4 \leq R_d$ (L kg^{-1}) $\leq 2.6 \times 10^5$), as expected for the predicted predominance of Pu(IV) (see Section 3.3). We note that the strength of the sorption follows the order Pu(IV) > U(IV) > Th(IV), which is in line with the strength of the first hydrolysis of these tetravalent actinides, *i.e.*, $\log^*\beta^\circ_{(1,1)}$(Pu) = (0.6 ± 0.2), $\log^*\beta^\circ_{(1,1)}$(U) = −(0.54 ± 0.06), and $\log^*\beta^\circ_{(1,1)}$(Th) = −(2.5 ± 0.5).[26]

The uptake of Pu under oxidizing conditions ($2.0 \times 10^3 \leq R_d$ (L kg^{-1}) $\leq 3.5 \times 10^3$) is clearly weaker than the sorption observed in reducing systems, but still significantly stronger than the uptake observed for U(VI). Although data for the uptake of An(V) by the granite and biotite gneiss are not available, we speculate that these results probably reflect the co-existence of Pu(V) and Pu(IV) under the experimental (pe + pH) conditions.

As the S/L ratio decreases, the R_d value rises. This can be attributed to the influence of the filter used during phase separation. However, tests conducted under identical

Table 7: Summary of the R_d values determined in this work for the uptake of U and Pu by granite and biotite gneiss under oxidizing (air) and reducing (HQ, $Na_2S_2O_4$) conditions.

RN	Material	Redox condition	Expected oxid. state	S/L (g L^{-1})	R_d (L kg^{-1}) (KAIST)	R_d (L kg^{-1}) (KIT)
Eu	Granite	Oxid. (air)	+III	1	$(1.2 \pm 0.1) \times 10^3$	–
	Biotite gneiss	Oxid. (air)	+III	1	$(1.7 \pm 0.3) \times 10^3$	–
	Granite	Oxid. (air)	+III	10	$(1.7 \pm 0.1) \times 10^2$	–
	Biotite gneiss	Oxid. (air)	+III	10	$(5.6 \pm 2.7) \times 10^2$	–
Th	Granite	Oxid. (air)	+IV	0.2	$(3.3 \pm 1.5) \times 10^3$	–
	Biotite gneiss	Oxid. (air)	+IV	0.2	$(4.1 \pm 1.2) \times 10^4$	–
	Granite	Oxid. (air)	+IV	1	$(1.2 \pm 1.6) \times 10^3$	–
	Biotite gneiss	Oxid. (air)	+IV	1	$(1.1 \pm 0.3) \times 10^4$	–
	Granite	Oxid. (air)	+IV	10	$(8.2 \pm 4.2) \times 10^2$	–
	Biotite gneiss	Oxid. (air)	+IV	10	$(4.7 \pm 2.3) \times 10^3$	–
U	Granite	Oxid. (air)	+VI	5	(16 ± 2)	(69 ± 32)
	Biotite gneiss	Oxid. (air)	+VI	5	(27 ± 5)	(78 ± 62)
	Granite	Oxid. (air)	+VI	50	(59 ± 8)	(16 ± 1)
	Biotite gneiss	Oxid. (air)	+VI	50	(44 ± 3)	(2 ± 1)
	Granite	Red. ($Na_2S_2O_4$)	+IV	0.2	–	$(1.2 \pm 0.5) \times 10^5$
	Biotite gneiss	Red. ($Na_2S_2O_4$)	+IV	0.2	–	$(3.9 \pm 1.1) \times 10^4$
	Granite	Red. ($Na_2S_2O_4$)	+IV	1	–	$(3.9 \pm 2.7) \times 10^3$
	Biotite gneiss	Red. ($Na_2S_2O_4$)	+IV	1	–	$(7.3 \pm 4.0) \times 10^3$
Pu	Granite	Oxid. (air)	+IV/+V	50	–	$(2.0 \pm 0.7) \times 10^3$
	Biotite gneiss	Oxid. (air)	+IV/+V	50	–	$(3.5 \pm 0.3) \times 10^3$
	Granite	Red. (HQ)	+IV	1	–	$(5.9 \pm 3.5) \times 10^4$
	Biotite gneiss	Red. (HQ)	+IV	1	–	$(2.6 \pm 1.6) \times 10^5$
	Granite	Red. (HQ)	+IV	10	–	$(3.1 \pm 0.1) \times 10^4$
	Biotite gneiss	Red. (HQ)	+IV	10	–	$(1.6 \pm 0.7) \times 10^4$
	Granite	Red. ($Na_2S_2O_4$)	+IV	10	–	$(2.0 \pm 1.1) \times 10^4$
	Biotite gneiss	Red. ($Na_2S_2O_4$)	+IV	10	–	$(2.8 \pm 0.8) \times 10^4$

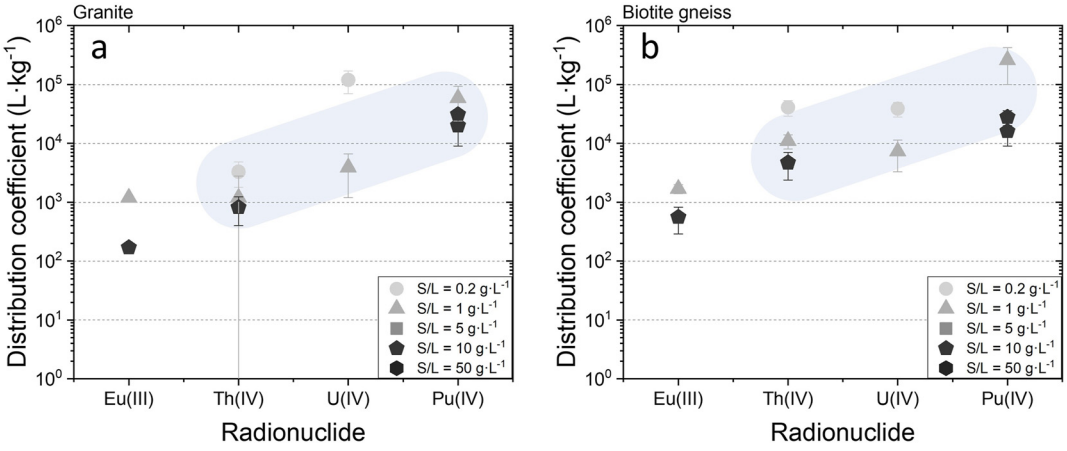

Figure 4: Distribution coefficients (R_d) of Eu(III) and tetravalent actinides (Th(IV), U(IV), and Pu(IV) represented by shaded elliptical areas) on granite (a) and biotite gneiss (b). Eu(III) and Th(IV) were sorbed under oxidizing conditions, while U(IV) and Pu(IV) were sorbed under reducing conditions. The darker the shape, the larger the S/L ratio.

groundwater conditions without the presence of solid phases showed that the filter had no significant effect. Therefore, this phenomenon is better interpreted as an increase in sorption efficiency caused by higher aqueous concentrations, which resulted from the reduction in available sorption sites.

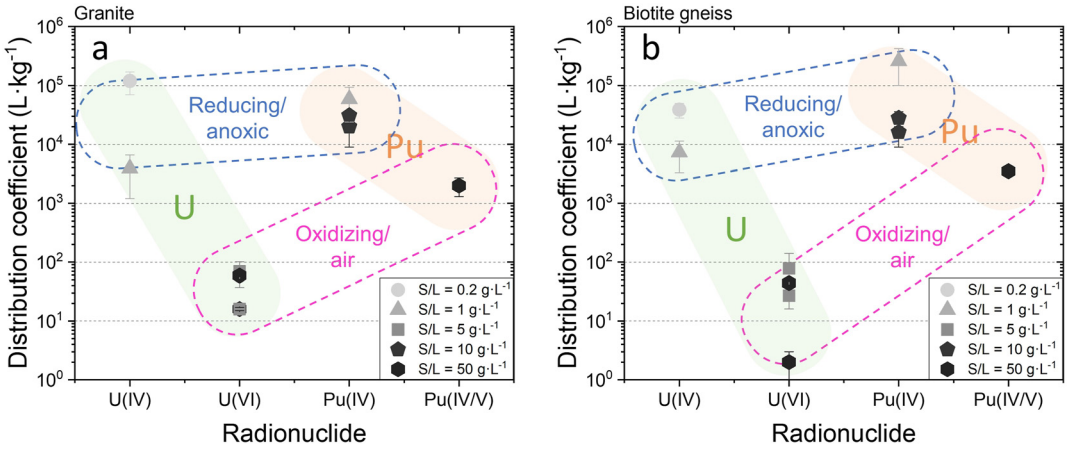

Figure 5: Distribution coefficients (R_d) of U and Pu on granite (a) and biotite gneiss (b). U(VI) and Pu(IV/V) were sorbed under oxidizing conditions, while U(IV) and Pu(IV) were sorbed under reducing conditions. The darker the shape, the larger the S/L ratio.

3.5 Comparison with sorption data available in the literature

This section compares the R_d values determined in this work for the uptake of Eu, Th, U and Pu by granite and gneiss under well-defined redox conditions with sorption data available in the literature for that have used similar sorbents. The core of the comparison focuses on the radionuclide migration parameters for the geosphere selected by POSIVA for the Safety Case for the disposal of spent nuclear fuel at Olkiluoto in Finland.[22] This choice is motivated by the similarities with the granite and gneiss materials considered by POSIVA (Table S1 in the Supplementary Material), as well as by the similarities with the groundwaters evaluated, in particular the fresh groundwaters labelled as ALL, ALLMO, and ALLMR (Table S2 in the Supplementary Material). The particle size distribution characterized after the milling of granodiorite and mica gneiss materials from Olkiluoto resulted in *ca.* 90 % of the sample with <250 µm and *ca.* 40 % with <90 µm. Key references mostly in the Korean context are also taken into account in this comparison, but it is out of the scope of this work to provide a complete overview of literature data on the uptake of radionuclides by granitic materials.

On the basis of the work by Puukko, Olin and co-workers, Hakanen et al. reported distribution ratios ranging from 2.5×10^3 L kg^{-1} to 7.0×10^3 L kg^{-1} for the uptake of Eu(III) by granodiorite and mica gneiss in fresh groundwaters with pH values of ~6.5 and ~7. [22,49,50] These values are in line with the distribution ratios quantified in this work for the Korean granite and biotite gneiss materials. ^{152}Eu autoradiographs conducted by Puukko and co-workers indicated that the uptake of Eu is dominated by micaceous minerals, mainly biotite.[50] Note that biotite is present in the biotite gneiss material investigated in this work but not in granite, which may explain the systematically higher R_d values determined for the uptake of Eu(III) by the former rock material. Baik and co-workers investigated the uptake of Eu(III) by granite within the pH range 3–10.[51] Experiments were performed at S/L = 50 g L^{-1} under aerobic (P_{CO_2} = 3.13 × 10^{-4} atm) and anaerobic (P_{CO_2} < 10^{-6} atm) conditions. Besides quartz (41.6–46.8 %), plagioclase (24.2–26.6 %) and K-feldspar (10.6–12.4 %), the granitic material used by the authors contained 12.8–16.6 % of biotite. The fraction 150–300 µm was used for preparation of the sorption samples. At pH ≈ 8.5, the authors reported similar R_d values for aerobic ($R_d \approx 1 \times 10^3$ L kg^{-1}) and anaerobic ($R_d \approx 1.5 \times 10^3$ L kg^{-1}) conditions. The slight differences in the distribution ratio were explained by changes in the aqueous speciation, *i.e.*, with the predominance of Eu(III)-carbonate complexes under aerobic conditions. Data reported by Baik and co-workers are in moderate agreement with the results obtained in this work, considering the differences between both experimental set-ups, *e.g.*, S/L ratio or size fraction of the granitic material used in the experiments.

Hakanen and co-workers reported distribution ratios for the uptake of Th(IV) by granite ($R_d \approx 7.0 \times 10^2$ L kg^{-1}) and gneiss ($3 \times 10^3 \leq R_d$ (L kg^{-1}) $\leq 4 \times 10^4$) materials in contact with fresh groundwater at pH 8.5–9 and slightly higher carbonate concentration compared to this work (1.1×10^{-3} M *vs.* 1.8×10^{-4} M).[22] These R_d values are in line with those determined in the present work for granite and biotite gneiss, showing a stronger uptake for gneiss than granite materials. All gneiss materials were characterized by a moderate content of biotite (8–23 % in Hakanen et al.,[22] 16.6 % in this work), whereas the presence of biotite in the granite materials was negligible (0.9 % in Hakanen et al.,[22] not detected in this work).

Experiments conducted by Hakanen and co-workers for the uptake of U(VI) by granite and gneiss materials contacted with fresh reference water (ALLMR) at pH ≈ 7–9 resulted in $60 \leq R_d$ (L kg^{-1}) $\leq 3 \times 10^2$.[22] The authors stated that "*No sorption data where the uranium oxidation state is convincingly shown to be solely U(IV) for crystalline rocks exist in the open literature*", and proposed to use the analogy with Th(IV) for the estimation of R_d values of U(IV), which according to linear-free energy relationships (LFER) should be greater than for Th(IV). Distribution coefficients reported by Hakanen et al.[22] for U(VI), and LFER estimates proposed for U(IV) are in line with the data obtained in the present work under oxidizing (air) and reducing (Ar-glovebox, $Na_2S_2O_4$, pe + pH ≈ 0.5) conditions, respectively. Baik and Hahn investigated the uptake of U(VI) by a granitic material[52] under analogous conditions as described above for Eu(III).[51] At pH = 6.9, the authors reported R_d values ranging from ~60 to ~18 L kg^{-1} at S/L ranging from 12.5 to 200 g L^{-1}, respectively. X-ray image mapping conducted by the same authors indicated that U is preferably associated to chlorite, although this phase is only found as a minor fraction in the investigated granite material.[53]

Kulmala and co-workers studied the sorption of Pu on rocks in groundwaters from three Finnish sites investigated by POSIVA (Olkiluoto, Romuvaara, and Kivetty).[54] This study served as the basis for the selection of K_d values by Hakanen et al. in the context of the Safety Case for the disposal of spent nuclear fuel at Olkiluoto.[22] Several materials were investigated, including granite and mica gneiss. A detailed description of the mineralogy of these materials and the composition of the groundwaters investigated is provided in Tables S3 and S4 of the Supplementary Material. Sorption experiments were performed both under oxic (air) or anoxic (N_2 atmosphere) conditions. Under oxic conditions, distribution ratios reported by the authors for non-saline systems (Romuvaara and Kivetty sites) ranged between 1×10^2 and 2×10^3 L kg^{-1}. Although the authors do not refer to the oxidation state of Pu, it is likely that these values do not correspond to Pu(IV) but rather to higher oxidation states of Pu, either +V or +VI. We note that the range of R_d values reported by Kulmala et al. under oxic conditions overlaps with the distribution ratios determined in this work. Slightly higher R_d values were reported by the authors for the uptake of Pu under anoxic conditions where the +IV oxidation state is expected to prevail ($4 \times 10^2 \leq R_d$ (L kg^{-1}) $\leq 9.1 \times 10^3$). These values are lower than those determined in this work under reducing conditions. We hypothesize that this could be caused by the significantly greater S/L ratio used in Kulmala et al.[54] (100 g L^{-1}), compared to those used in the present work (1 and 10 g L^{-1}).

4 Conclusions

A comprehensive batch sorption study was performed on the uptake of $^{(151+153)}$Eu, ^{232}Th, ^{238}U, and ^{242}Pu by Korean granite and biotite gneiss. Experiments were performed under oxidizing (air) and reducing (set by HQ or $Na_2S_2O_4$) conditions, which impact the oxidation state of ^{238}U and ^{242}Pu thus their sorption properties. Experimental conditions ($[RN]_0$ and S/L ratio) were selected on the basis of scoping speciation and solubility calculations using the NEA-TDB thermodynamic database and K_d values available in the literature for the uptake of these radionuclides by granitic materials. The values of pH, E_h, and [RN] were measured at 20 days and 113 days after the addition of the radionuclides. The combination of experimentally measured (pe + pH) and calculated *Pourbaix* diagrams of U and Pu under the conditions of the experiments ([Ca], C_{tot}, ionic strength) predicts the predominance of U(VI) and U(IV) under oxidizing and reducing conditions, respectively. In the case of Pu, the +IV oxidation state is expected to predominate in all investigated reducing systems, whereas experimental (pe + pH) values and calculated *Pourbaix* diagrams indicate the possible coexistence of Pu(IV) and Pu(V) under oxidizing conditions.

A strong sorption is quantified for U and Pu under reducing conditions, with R_d values in the range of $\approx 1 \times 10^3$–1×10^4 L kg^{-1} and $\approx 1 \times 10^4$–1×10^5 L kg^{-1}, respectively. A weaker uptake is observed for Pu under oxidizing conditions ($R_d \approx 1 \times 10^3$ L kg^{-1}), which possibly reflects the co-existence of Pu(IV) and Pu(V). As foreseen, considering the weaker strength of U(VI) hydrolysis compared to U(IV), U(VI) prevailing in oxidizing systems shows the weakest sorption of all investigated systems $R_d \approx 2$–70 L kg^{-1}.

The results obtained in this work show a moderate to strong sorption of Eu, Th, U, and Pu in the granite and biotite gneiss materials investigated. The strength of the uptake is strongly dependent on the redox conditions, which impact the redox speciation of U/Pu and accordingly their chemical behavior. These observations emphasize the importance of conducting sorption experiments with the relevant redox-sensitive actinides (*e.g.*, U, Np, Pu) under well-controlled conditions, in addition to the work with redox stable probes (*e.g.*, Th). These results highlight as well the importance of an accurate knowledge of the redox conditions in a given geochemical context.

Acknowledgements: Max Bachert and Jonas Rentmeister (both KIT-INE) are kindly acknowledged for the SF-ICP-MS and TIC measurements.

Research ethics: Not applicable.
Informed consent: Not applicable.
Author contributions: The authors have accepted responsibility for the entire content of this manuscript and approved its submission.
Use of Large Language Models, AI and Machine Learning Tools: None declared.
Conflict of interest: The authors state no conflict of interest.
Research funding: This work was funded by Hyundai Engineering and Construction Co. Ltd, the Institute for Korea Spent Nuclear Fuel (iKSNF) and Korea Institute of Energy Technology Evaluation and Planning (KETEP) grant funded by the Korea government Ministry of Trade, Industry and Energy (MOTIE) (No. 1415176399, iKSNF_2021040101003C, and RS-2023-00236697).
Data availability: The raw data can be obtained on request from the corresponding authors.

References

1. Ewing, R. C. Less Geology in the Geological Disposal of Nuclear Waste. *Science* **1999**, *286*, 415–417.
2. SKB. *R&D-Programme 2004 – Programme for Research, Development and Demonstration of Methods for the Management and Disposal of Nuclear Waste, Including Social Science Research*. SKB Report TR-04-21, 2004.
3. Cho, W.-J.; Kwon, S.; Park, J.-H.. KURT a Small-Scale Underground Research Laboratory for the Research on a High-Level Waste Disposal. *Ann. Nucl. Energy* **2008**, *35*, 132–140.
4. Tsuruta, T.; Tagami, M.; Amano, K.; Matsuoka, T.; Kurihara, A.; Yamada, Y.; Koike, K. Geological Investigations for Geological Model of Deep Underground Geoenvironment at the Mizunami Underground Research Laboratory (MIU). *J. Geol. Soc. Jpn.* **2013**, *119*, 59–74.
5. Wang, J.; Chen, L.; Su, R.; Zhao, X. The Beishan Underground Research Laboratory for Geological Disposal of High-Level Radioactive Waste in China. *J. Rock Mech. Geotech. Eng.* **2018**, *10*, 411–435.
6. Vieno, T.; Nordman, H. *Safety Assessment of Spent Fuel Disposal in Hästholmen, Kivetty, Olkiluoto and Romuvaara TILA-99*. Posiva Report 99-07, 1999.
7. Hagues, A. W.; Williams, M. M. R.; Eaton, M. D. A Probabilistic Study of the Effect of Retardation Factor Uncertainty Using a Compartment Model for Radionuclide Release into the Biosphere. *Ann. Nucl. Energy* **2010**, *37*, 1197–1207.
8. Kwon, S.; Cho, W. J. Rock Mechanics Studies at the KAERI Underground Research Tunnel for High-Level Radioactive Waste Disposal. *Tunn. Undergr. Space* **2007**, *17*, 43–55.
9. Lee, J.-H.; Jung, H.; Cheong, J.-Y.; Park, J.-W.; Yun, S.-T. Evaluation of Groundwater Quality in Crystalline Bedrock Site for Disposal of Radioactive Waste. *J. Nucl. Fuel Cycle Waste Technol.* **2014**, *12*, 275–286.
10. Cheon, D.-S.; Jin, K.; Synn, J. H.; Kihm, Y. H.; Jeon, S. Preliminary Study on Candidate Host Rocks for Deep Geological Disposal of HLW Based on Deep Geological Characteristics. *Tunn. Undergr. Space* **2024**, *34*, 28–53.
11. Hedin, A.; Olsson, O. Crystalline Rock as a Repository for Swedish Spent Nuclear Fuel. *Elements* **2016**, *12*, 247–252.
12. Nguyen, T. S. Progressive Damage of a Canadian Granite in Laboratory Compression Tests and Underground Excavations. *Minerals* **2021**, *11*, 10.
13. Pradhan, R. M.; Singh, A.; Ojha, A. K.; Biswal, T. K. Structural Controls on Bedrock Weathering in Crystalline Basement Terranes and its Implications on Groundwater Resources. *Sci. Rep.* **2022**, *12*, 11815.
14. Geckeis, H.; Lützenkirchen, J.; Polly, R.; Rabung, T.; Schmidt, M. Mineral–water Interface Reactions of Actinides. *Chem. Rev.* **2013**, *113*, 1016–1062.
15. Stuckless, J. S.; Nkomo, I. T. Uranium-Lead Isotope Systematics in Uraniferous Alkali-Rich Granites From the Granite Mountains, Wyoming; Implications for Uranium Source Rocks. *Econ. Geol.* **1978**, *73*, 427–441.
16. Tieh, T. T.; Ledger, E. B.; Rowe, M. W. Release of Uranium from Granitic Rocks During In Situ Weathering and Initial Erosion (Central Texas). *Chem. Geol.* **1980**, *29*, 227–248.
17. Terekhov, E. N.; Shcherbakova, T. F. Genesis of Positive Eu Anomalies in Acid Rocks From the Eastern Baltic Shield. *Geochem. Int.* **2006**, *44*, 439–455.
18. Ranjan, S.; Upadhyay, D.; Abhinay, K.; Srikantappa, C. Paleoarchean and Neoarchean Tonalite–Trondhjemite–Granodiorite (TTG) and Granite Magmatism in the Western Dharwar Craton, Southern India: Implications for Archean Continental Growth and Geodynamics. *Precambrian Res*. **2020**, *340*, 105630.
19. Lee, S. G.; Lee, K. Y.; Cho, S. Y.; Yoon, Y. Y.; Kim, Y. Sorption Properties of ^{152}Eu and ^{241}Am in Geological Materials: Eu as an Analogue for Monitoring the Am Behaviour in Heterogeneous Geological Environments. *Geosci. J.* **2006**, *10*, 103–114.
20. Hwang, J.; Moon, S.-H.; Ripley, E. M.; Kim, Y. H. Determining Uraniferous Host Rocks and Minerals as a Source of Dissolved Uranium in Granite Aquifers Near the Central Ogcheon Metamorphic Belt, Korea. *Environ. Earth. Sci.* **2014**, *72*, 4035–4046.
21. Hwang, J.; Moon, S.-H. Geochemical Evidence for K-Metasomatism Related to Uranium Enrichment in Daejeon Granitic Rocks Near the Central Ogcheon Metamorphic Belt. *Korea. Geosci. J.* **2018**, *22*, 1001–1013.
22. Hakanen, M.; Ervanne, H.; Puukko, E. *Safety Case for the Disposal of Spent Nuclear Fuel at Olkiluoto: Radionuclide Migration Parameters for the Geosphere*. Posiva Report 2012-41, 2014.
23. Metz, V.; Geckeis, H.; González-Robles, E.; Loida, A.; Bube, C.; Kienzler, B. Radionuclide Behaviour in the Near-Field of a Geological Repository for Spent Nuclear Fuel. *Radiochim. Acta* **2012**, *100*, 699–713.
24. Altmaier, M.; Gaona, X.; Fanghänel, T. Recent Advances in Aqueous Actinide Chemistry and Thermodynamics. *Chem. Rev.* **2013**, *113*, 901–943.
25. Çevirim-Papaioannou, N. Redox Chemistry, Solubility and Hydrolysis of Uranium in Dilute to Concentrated Salt Systems. Ph.D. Thesis; Karlsruhe Institute of Technology: Germany, **2018**.
26. Grenthe, I.; Gaona, X.; Plyasunov, A. V.; Rao, L.; Runde, W. H.; Grambow, B.; Konings, R. J. M.; Smith, A. L.; Moore, E. E. *Second Update on the Chemical Thermodynamics of Uranium, Neptunium, Plutonium, Americium and Technetium*; OECD/NEA Chemical Thermodynamics: Boulogne-Billancourt, France, Vol. 14, 2020.
27. Neck, V.; Altmaier, M.; Fanghänel, T. Solubility of Plutonium Hydroxides/hydrous Oxides Under Reducing Conditions and in the Presence of Oxygen. *Comptes Rendus Chim.* **2007**, *10*, 959–977.
28. Tasi, A.; Gaona, X.; Fellhauer, D.; Böttle, M.; Rothe, J.; Dardenne, K.; Schild, D.; Grivé, M.; Colàs, E.; Bruno, J.; Källström, K.; Altmaier, M.; Geckeis, H. Redox Behavior and Solubility of Plutonium Under Alkaline, Reducing Conditions. *Radiochim. Acta* **2018**, *106*, 259–279.

29. Demnitz, M.; Schymura, S.; Neumann, J.; Schmidt, M.; Schäfer, T.; Stumpf, T.; Müller, K. Mechanistic Understanding of Curium(III) Sorption on Natural K-Feldspar Surfaces. *Sci. Total Environ.* **2022**, *843*, 156920.
30. Iida, Y.; Yamaguchi, T.; Tanaka, T.; Hemmi, K. Sorption Behavior of Thorium Onto Granite and its Constituent Minerals. *J. Nucl. Sci. Technol.* **2016**, *53*, 1573–1584.
31. Kitamura, A.; Yamamoto, T.; Nishikawa, S.; Moriyama, H. Sorption Behavior of Am(III) Onto Granite. *J. Radioanal. Nucl. Chem.* **1999**, *239*, 449–453.
32. Baik, M. H.; Hyun, S. P.; Hahn, P. S. Surface and Bulk Sorption of Uranium (VI) Onto Granite Rock. *J. Radioanal. Nucl. Chem.* **2003**, *256*, 11–18.
33. Keum, D. K.; Choi, B. J.; Baik, M. H.; Hahn, P. S. Uranium (VI) Adsorption and Transport in Crushed Granite. *Environ. Eng. Res.* **2002**, *7*, 103–111.
34. Nebelung, C.; Brendler, V. U (VI) Sorption on Granite: Prediction and Experiments. *Radiochim. Acta* **2010**, *98*, 2010.
35. Alonso, U.; Missana, T.; Geckeis, H.; García-Gutiérrez, M.; Turrero, M. J.; Möri, R.; Schäfer, T.; Patelli, A.; Rigato, V. Role of Inorganic Colloids Generated in a High-Level Deep Geological Repository in the Migration of Radionuclides: Open Questions. *J. Iberian Geol.* **2006**, *32*, 79–94.
36. Fellhauer, D. Untersuchungen zur Löslichkeit und Redoxchemie von Plutonium und Neptunium. Ph.D. Thesis; Universität Heidelberg: Germany, **2013**.
37. Neill, T. S.; Morris, K.; Pearce, C. I.; Sherriff, N. K.; Burke, M. G.; Chater, P. A.; Janssen, A.; Natrajan, L.; Shaw, S. Stability, Composition, and Core-Shell Particle Structure of Uranium (IV)-Silicate Colloids. *Environ. Sci. Technol.* **2018**, *52*, 9118–9127.
38. Szabo, P.; Tasi, A.; Gaona, X.; Maier, A.; Hedström, S.; Altmaier, M.; Geckeis, H. Uptake of Ni(II), Eu(III) and Pu(III/IV) by Hardened Cement Paste in the Presence of Proxy Ligands for the Degradation of Polyacrylonitrile. *Front. Nucl. Eng.* **2023**, *2*, 1117413.
39. Tasi, A.; Gaona, X.; Rabung, T.; Fellhauer, D.; Rothe, J.; Dardenne, K.; Lützenkirchen, J.; Grivé, M.; Colàs, E.; Bruno, J.; Källström, K.; Altmaier, M.; Geckeis, H. Plutonium Retention in the Isosaccharinate–Cement System. *Appl. Geochem.* **2021**, *126*, 104862.
40. Eun, H.; Lee, S.; Lee, J.; Jeong, M.-S.; Iqbal, S.; Yun, J.-I. Kinetic and Competitive Effects of Sorption on Multi-Element Migration Through Crushed Granite and Biotite Gneiss in Ca-HCO_3-SO_4 Type Groundwater. *J. Environ. Radioact.* **2024**, *278*, 107501.
41. Neck, V.; Altmaier, M.; Seibert, A.; Yun, J.-I.; Marquardt, C. M.; Fanghänel, T. Solubility and Redox Reactions of Pu(IV) Hydrous Oxide: Evidence for the Formation of PuO_{2+x}(s, Hyd). *Radiochim. Acta* **2007**, *95*, 193–207.
42. Tasi, A.; Gaona, X.; Fellhauer, D.; Böttle, M.; Rothe, J.; Dardenne, K.; Polly, R.; Grivé, M.; Colàs, E.; Bruno, J.; Källström, K.; Altmaier, M.; Geckeis, H. Thermodynamic Description of the Plutonium-α-D-Isosaccharinic Acid System I: Solubility, Complexation and Redox Behavior. *Appl. Geochem.* **2018**, *98*, 247–264.
43. Yalçıntaş, E.; Gaona, X.; Scheinost, A. C.; Kobayashi, T.; Altmaier, M.; Geckeis, H. Redox Chemistry of Tc(VII)/Tc(IV) in Dilute to Concentrated NaCl and $MgCl_2$ Solutions. *Radiochim. Acta* **2015**, *103*, 57–72.
44. Altmaier, M.; Gaona, X.; Fellhauer, D.; Buckau, G. *Intercomparison of Redox Determination Methods on Designed and Near-Natural Aqueous Systems*. KIT-SR 7572, 2010.
45. Tan, S. H.; Horlick, G. Matrix-Effect Observations in Inductively Coupled Plasma Mass Spectrometry. *J. Anal. At. Spectrom.* **1987**, *2*, 745–763.
46. Ahlrichs, R.; Furche, F.; Grimme, S. Comment on "Assessment of Exchange Correlation Functionals" [AJ Cohen, NC Handy, Chem. Phys. Lett., 316 (2000) 160–166];. *Chem. Phys. Lett.* **2000**, *325*, 317–321.
47. Bruno, J.; González-Siso, M. R.; Duro, L.; Gaona, X.; Altmaier, M. Key Master Variables Affecting the Mobility of Ni, Pu, Tc and U in the Near Field of the SFR Repository. In *Main Experimental Findings and PA Implications of the PhD Thesis*. SKB Report TR18-01, SKB, Solna, Sweden, 2018.
48. Xie, Y.; Shao, D.; Lu, X.; Hayat, T.; Alharbi, N. S.; Chen, C.; Song, G.; Chen, D.; Sun, Y. Spectroscopic Investigation of Enhanced Adsorption of U(VI) and Eu(III) on Magnetic Attapulgite in Binary System. *Ind. Eng. Chem. Res.* **2018**, *57*, 7533–7543.
49. Olin, M.; Puukko, E.; Puhakka, E.; Hakanen, M.; Lindberg, A.; Lehikoinen, J. Sorption of Biotite. In *4th Annual Workshop Proceedings of the Integrated Project "Fundamental Processes of Radionuclide Migration" (6th EC FP IP FUNMIG)*, 2009; pp. 335–343.
50. Puukko, E.; Puhakka, E.; Lindberg, A.; Olin, M.; Hakanen, M.; Lehikoinen, J. Mineral-Specific Sorption of Cs, Ni, Eu and Am on Granodiorite and Mica Gneiss. In *1st Annual Workshop of Integrated Project "Fundamental Processes of Radionuclide Migration" (IP FUNMIG)*, 2006; pp. 80–85.
51. Baik, M. H.; Cho, W. J.; Hahn, P. S. Effects of Speciation and Carbonate on the Sorption of Eu(III) Onto Granite. *Environ. Eng. Res.* **2004**, *9*, 160–167.
52. Baik, M. H.; Hahn, P. S. An Experimental Study on the Sorption of U(VI) Onto Granite. *Nucl. Eng. Technol.* **2002**, *34*, 445–454.
53. Baik, M. H.; Hyun, S. P.; Cho, W. J.; Hahn, P. S. Contribution of Minerals to the Sorption of U(VI) on Granite. *Radiochim. Acta* **2004**, *92*, 663–669.
54. Kulmala, S.; Hakanen, M.; Lindberg, A. *Sorption of Plutonium on Rocks in Groundwaters From Posiva Investigation Sites*. Posiva Report 98-12, 1998.